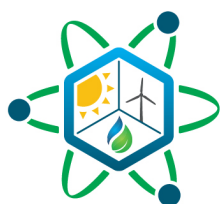


# Follow-On Status Report on FY2022 Model Development within the Integrated Energy Systems HYBRID Repository

April | 2022

**Daniel Mikkelson**  
**Amey Shigrekar**  
**Konor L Frick**  
**Aaron Epiney**  
***Idaho National Laboratory***



# IES

Integrated Energy Systems

#### **DISCLAIMER**

This information was prepared as an account of work sponsored by an agency of the U.S. Government. Neither the U.S. Government nor any agency thereof, nor any of their employees, makes any warranty, expressed or implied, or assumes any legal liability or responsibility for the accuracy, completeness, or usefulness, of any information, apparatus, product, or process disclosed, or represents that its use would not infringe privately owned rights. References herein to any specific commercial product, process, or service by trade name, trade mark, manufacturer, or otherwise, does not necessarily constitute or imply its endorsement, recommendation, or favoring by the U.S. Government or any agency thereof. The views and opinions of authors expressed herein do not necessarily state or reflect those of the U.S. Government or any agency thereof.

# **Status Report on FY2022 Model Development within the Integrated Energy Systems HYBRID Repository**

**Daniel Mikkelson  
Amey Shigrekar  
Konor L Frick  
Aaron Epiney**  
*Idaho National Laboratory*

**April 2022**

**Idaho National Laboratory  
Integrated Energy Systems  
Idaho Falls, Idaho 83415**

**<http://www.ies.inl.gov>**

**Prepared for the  
U.S. Department of Energy  
Office of Nuclear Energy  
Under DOE Idaho Operations Office  
Contract DE-AC07-05ID14517**

*Page intentionally left blank*

## **ABSTRACT**

This publication details newly created energy storage and reactor models developed within the HYBRID modeling repository as part of the Department of Energy Office of Nuclear Energy's (DOE-NE) Integrated Energy Systems (IES) program, led by Idaho National Laboratory (INL).

Recently, model development has included the creation of three dynamic systems-level models in the IES-based HYBRID repository: a pebble bed high temperature gas reactor (HTGR), compressed air energy storage (CAES), and Modelica-Standard-Library-based two-tank sensible heat storage (SHS). The models are developed using the latest publicly available data and they incorporate the possibility of control strategy inclusion for use with the existing IES modeling, analysis, and optimization toolset. Simulations have showcased the abilities of each technology to flexibly operate in ways consistent the expectations for IES operation.

Once these models are made available, they can be utilized within different integrated energy park concepts in order to understand optimal system operation, control, and dispatching. Moreover, given the generic nature of the models, industrial partner technologies can be quickly added to the repository by using the existing models as a basis. Additional dynamic models for thermal energy storage concepts can be developed and added to the HYBRID repository as needed.

*Page intentionally left blank*

## CONTENTS

ABSTRACT.....	iii
LIST OF ACRONYMS, INITIALISMS, AND ABBREVIATIONS.....	viii
1. INTRODUCTION.....	1
2. HIGH TEMPERATURE GAS REACTOR.....	3
2.1 Model Development.....	3
2.1.1 HTGR Rankine Cycle.....	3
2.1.2 Primary Model Design.....	3
2.2 HTGR Rankine Model Results.....	5
2.2.1 Steady-state System Results.....	5
2.3 Additional Planned Work.....	5
3. COMPRESSED AIR ENERGY STORAGE (CAES).....	6
3.1 Model Development.....	6
3.1.1 CAES Technology Background.....	6
3.1.2 Primary Model Design.....	7
3.2 CAES Preliminary Results.....	9
3.2.1 Charging and Storage Mode.....	9
3.2.2 Discharging Mode.....	10
3.3 Additional Planned Work.....	11
4. Two-tank Sensible Heat Storage.....	12
4.1 Model Development.....	12
4.1.1 Storage Two-Tank Loop Design.....	12
4.1.2 Integration Design.....	14
4.2 Two-Tank Test Results.....	14
4.2.1 Stand-Alone System Results.....	14
4.3 Additional Planned Work.....	17
5. CONCLUSIONS.....	17
6. ACKNOWLEDGEMENTS.....	18
7. REFERENCES.....	18

## FIGURES

Figure 1. Example architecture for an Integrated Energy System.....	1
Figure 2. HYBRID logo.....	2
Figure 3. Rankine HTGR primary side design in HYBRID repository.....	3
Figure 4. HTGR Rankine secondary side design in HYBRID repository.....	4
Figure 5. Schematic of a CAES power plant [8].....	6
Figure 6. Charging cycle in the CAES model.....	7
Figure 7. Discharging cycle of the CAES model.....	8
Figure 8. Cavern pressure and temperature during the charging cycle.....	9
Figure 9. Pressure and temperature profile in the cavern during the storage mode.....	10
Figure 10. Cavern pressure and temperature profile during the discharge cycle.....	11
Figure 11. Model diagram of a sensible heat system.....	13
Figure 12. Control system model for the current standard SHS test.....	13
Figure 13. Hot and cold tank levels throughout the 10-day cycle. Hysteresis initiation and shutdown signals are included for reference.....	15
Figure 14. Discharging and charging power as measured within the heat exchangers.....	15
Figure 15. Charging mass flow rate on the storage side (red) along with the steam input (blue). Note that there is a 2 kg/s circulating flow on the steam side of the charging heat exchanger.....	15
Figure 16. Discharge mass flow rate during the simulation.....	16
Figure 17. Steam production rate through the simulation. The demand during the discharging period is nominally 1.5kg/s.....	16
Figure 18. Discharge mass flow rate and normalized steam flow rate during a discharging cycle. ....	16
Figure 19. Hot and cold tank temperature profiles throughout the 10-day session. Charging mass flow is added (not-zeroed) to indicate charging periods.....	17

## TABLES

Table I. Comparison of HTGR Rankine steady state results between reference and simulation values. Bolded physical variables indicate the value is controlled.....	5
---	---



*Page intentionally left blank*

## **LIST OF ACRONYMS**

CAES	Compressed Air Energy Storage
FORCE	Framework for Optimization of Resources and Economics
HTGR	High Temperature Gas Reactor
IES	Integrated Energy Systems
INL	Idaho National Laboratory
SHS	Sensible Heat Storage

# 1. INTRODUCTION

The need for modernization within the electrical grid has become a national and global priority. Domestically, the Department of Energy has developed a program, the Energy Storage Grand Challenge, to “accelerate the development, commercialization, and utilization of next-generation energy storage technologies and sustain American global leadership in energy storage.” The program’s aggressive goal is to develop storage technologies capable of meeting all market demands by the year 2030 [1]. The ability to store thermal, electrical, and chemical energy at the grid-participant level will enable energy producers to more dynamically allocate their energy as needed across multiple applications. For some resources, this paradigm shift would lead to continuous energy application despite intermittent generation; and for some, the inverse may be true, with energy being stored up during continuous generation and then applied later in batches. In either case, innovations in electrical, mechanical, thermal, chemical, and electro-chemical energy storage technologies are for providing the maximum safety, economic, and environmental flexibility.

The Department of Energy Office of Nuclear Energy’s Integrated Energy Systems (IES) program, led by Idaho National Laboratory (INL), continues to spearhead research, development, and demonstration efforts to produce analytic tools and determine technology candidates, integration techniques and analysis methods. Because IES increase the number of markets in which energy producers and users can consume or direct energy streams, traditional methods that analyze standalone systems are no longer sufficient. Significant architecture development is required for new tools that can incorporate novel control strategies and balance complex production/demand systems that may include memory and operate within multiple systems’ safety limits requires significant architecture development. An example potential IES that integrates power generators, Figure 1 shows a potential IES with power generators, Hydrogen production, the electrical grid, and multiple Hydrogen users is shown in.

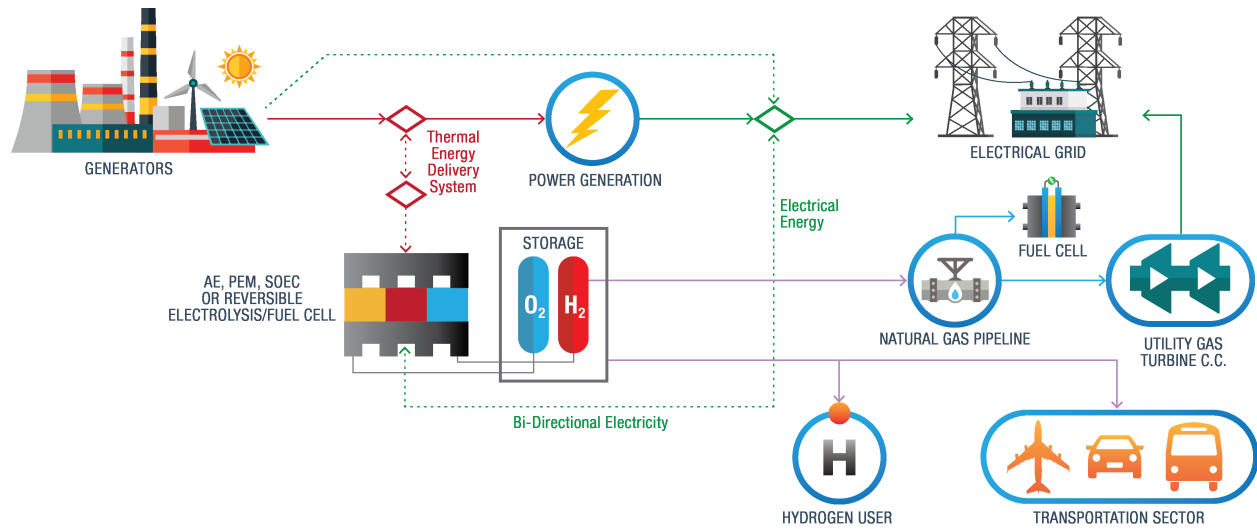


Figure 1. Example architecture for an Integrated Energy System.

One component of the IES architecture under development at INL is HYBRID, the new logo shown in Figure 2, a repository of process models that includes a library of high-fidelity process models written in the Modelica modeling language [2]. HYBRID is one analytic tool that will be integrated into the Framework for Optimization of ReCourses and Economics (FORCE) analysis framework. Modelica is a non-proprietary, object-oriented, equation-based language used to conveniently model complex, physical systems. It is also an inherently time-dependent modeling language that enables swift interconnection of independently developed models. Being an equation-based modeling language that employs differential algebraic equation solvers, it allows users to focus on the physics of a problem rather than the solving technique, thus fostering faster model generation and, ultimately, analysis. This feature, alongside model

flexibility, has led to widespread use of Modelica across various industries for commercial applications. System interconnectivity and the ability to quickly develop novel control strategies while still encompassing overall system physics are why INL has chosen to develop the IES framework in Modelica.

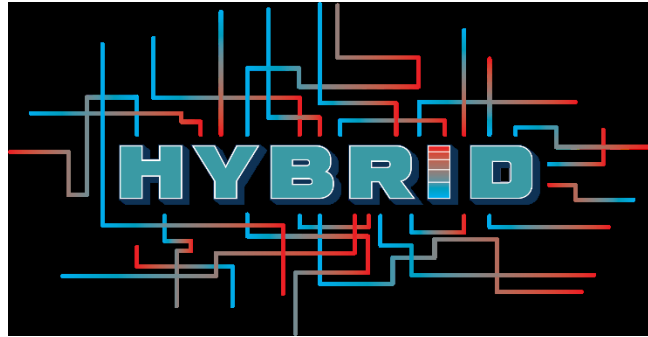


Figure 2. HYBRID logo.

Current models in INL's HYBRID repository includes ones for four-loop light water cooled nuclear power plants, natural-circulation small modular reactors, natural gas turbines, coal plants, switchyards, high-temperature steam electrolysis, reverse osmosis, electric grid models, concrete thermal energy storage, two tank sensible heat thermal energy storage, thermocline energy storage, and batteries. HYBRID also includes some IES examples using the developed models. A consistent structure is used throughout to facilitate control strategy studies.

This report details ongoing model development in support of IES research. It is a follow-up to a previous milestone report [2]. As the IES program looks forward, support for advanced reactors and a wide variety of energy storage technologies is needed. The models presented in this report include a high temperature gas reactor, compressed air energy storage (CAES), and two-tank sensible heat storage. All the models were implemented using the commercially available Modelica-based modeling and simulation environment (i.e., a Dynamic Modeling Laboratory version 2021x or 2022) [4]. Packages and open-source libraries that were developed in house were utilized to facilitate modeling and simulation. In particular, the Modelica standard library version 4.0 and TRANSFORM from Oak Ridge National Laboratory [5] [6].

## 2. HIGH TEMPERATURE GAS REACTOR

Much of the background and theory behind the core structure was covered in the previous milestone update published in December [2]. That milestone noted that future work on the HTGR design required two primary steps: a Rankine cycle system and prismatic-style fuel structure. The Rankine cycle system has now been further developed this document gives an update on the resulting progress.

### 2.1 Model Development

HTGR model development has continued to improve upon the Brayton cycle system as well as build up the Rankine cycle system. Both models presently use pebble bed core designs.

#### 2.1.1 HTGR Rankine Cycle

The IES program analysis team must be provided with a Rankine-system HTGR, since it represents the most advanced HTGR design currently in development. An example of this system is the Xe-100, which is being developed by X-Energy [7]. This system operates at about 125 MWt and 43.75 MWe. Exact control methods and values have been published in the reference documents. The system developed in HYBRID was able to mirror the control methods, but so far the model construction has failed to match the reference values.

#### 2.1.2 Primary Model Design

The Rankine cycle system was developed to match the structure of other reactor models within HYBRID. More specifically, the primary and secondary sides of the reactor were split into two models to allow for intermediate steam distribution modelings.

The primary side of the HTGR Rankine system is a relatively simple system seen, as seen in Figure 3. Heated gas flows out of the core and directly to the heat exchanger to produce steam. Downstream of the heat exchanger the flow travels through a circulating blower, basically a low-head, high-flow compressor before re-entering the core.

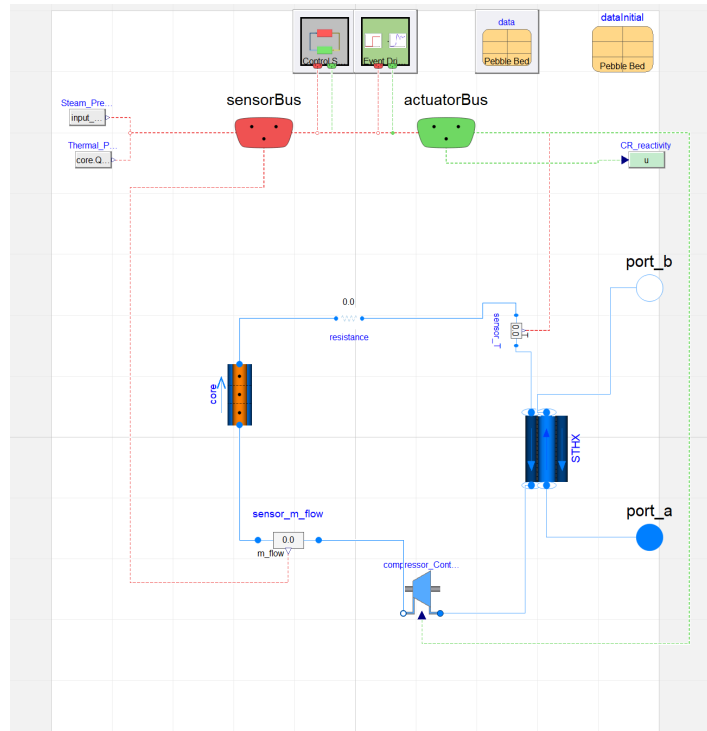


Figure 3. HTGR Rankine system primary-side design in the HYBRID repository.

In this case, the secondary-side is based on X-Energy's Xe-100 design. The HYBRID design is shown in Figure 4. Two turbine stages are modeled. After the first stage, a moisture separator directs any liquid content to mix and heat the feed flow sourced from the condenser. A valve downstream of the moisture separator – but still upstream of the second turbine stage – can bypass additional flow in order to preheat the feed flow to the desired temperature.

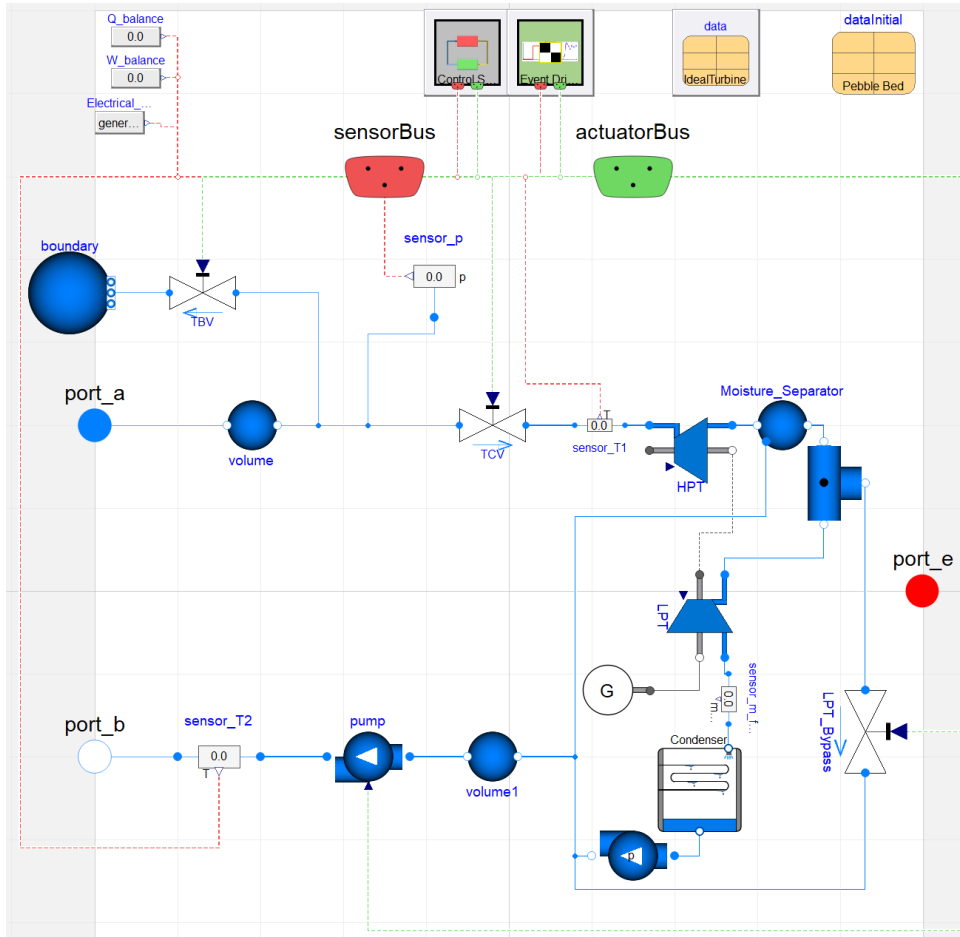


Figure 4. HTGR Rankine secondary side design in HYBRID repository.

One advantage of building a system for which a certain amount of literature is available is learning what the system's control system is expected to be. In this case, five controlled values initiate system changes. They are:

- Reactor coolant exit temperature, which drives control rod movement
- Steam exit temperature, which drives the feed water control pump
- Steam pressure, which drives the changes in the blower speed
- Feedwater temperature, which opens and closes the intermediate bypass valve between turbine stages
- Turbine power, which is governed by the turbine control valve

As of now, the steady state results are the primary values that can be compared. The published data do not include certain crucial geometric and thermal mass information necessary for comparing transient results.

## 2.2 HTGR Rankine Model Results

HTGR modeling has been able to successfully match some literature steady state modeling results of some older HTGR designs of a 125MWt and 43.75MWe system.

### 2.2.1 Steady-State System Results

The modeling results can be compared with those from the literature in order to ascertain the relative accuracy of the models constructed thus far [7]. Many of the values are controlled, and should therefore be completely identical in both the reference and HYBRID models. These values are included in Table I, along with some uncontrolled values.

Table I. Comparison of HTGR Rankine steady-state results from the reference and simulation values. **Bolded** physical variables indicate controlled values.

Physical Variable	Reference Value	Simulation Value	Simulation Error Relative to Reference
<b>Electric power (MW)</b>	43.75	43.62	-0.297%
Thermal power (MW)	125	122.0	-2.4%
<b>Steam temperature (°C)</b>	540	540	N/A
<b>Steam pressure (MPa)</b>	14.0	14.0	N/A
Steam mass flow rate (kg/s)	50	48.0	-4.0%
<b>Feedwater temperature (°C)</b>	208	208	N/A
Primary mass flow rate (kg/s)	47.5	48.4	-2.1%
<b>Core exit temperature (°C)</b>	750	750	N/A
Core inlet temperature (°C)	255	265	3.9%

The simulation and reference results match very closely on nearly all of the values. Additional work can be done to tune the system parameters such that the entire system matches. Differences in the assumed turbine model are likely the sources of difference between the two models. As the HYBRID turbine creates almost identical power with less steam flow, this difference propagates throughout the simulation. A lower steam mass flow rate reduces the amount of heat transferred through the primary steam generator, which results in less power in the nuclear core. Similarly, the reduction in power combined with a controlled core exit temperature leads to the difference in core inlet temperature value. Overall, the results match very closely.

## 2.3 Additional Planned Work

The HYBRID model must be tuned so as to better match the full results of the reference model. The reference model also includes some transient results, and additional tuning of the Hybrid model is needed to match those as well. The challenges in matching these values center around correctly tuning the control systems and sizing the physical components, especially in regard to obtaining accurate (as measured by the simulation results) thermal mass measures on the primary and secondary sides. Obtaining these values should lead to similar physical system derivatives.

A prismatic core design is still needed to complete the suite of HTGR models within the Hybrid repository. The prismatic design should be similar to existing light-water reactor core designs, so adapting existing models should be reasonably straightforward.

Expanding the set of control systems and IES designs should be another priority. Rankine cycle HTGRs may provide an opportunity to integrate thermal applications on the primary or secondary sides, and both possibilities should be investigated.

### 3. COMPRESSED AIR ENERGY STORAGE (CAES)

CAES is a technology that stores potential energy by compressing air during periods when electricity production exceeds demand. This compressed air can be stored in large underground reservoirs or tanks, and can be used to generate additional power via a gas turbine during peak electricity demands. Depending on the location of CAES, it may be possible to store sufficient energy for CAES to truly be a seasonal storage option for grid planners. During the discharge, energy production efficiency can be improved by adding some form of heat prior to producing power in the turbine.

#### 3.1 Model Development

CAES model development has progressed in stages so far with separate development of charging and discharging models. Modeling at zero-flow conditions can be challenging, especially for components that are designed only to operate at or near nominal conditions such as compressors and turbines. Results of separate charging and discharging models are included in this report.

##### 3.1.1 CAES Technology Background

A CAES system mainly consists of a compressor train, air reservoir, motor and generator, and turbine. Most designs also include a combustor, though a few designs that operate on a fuel-free principle. Figure 5 shows a simplified schematic of a CAES system with a combustor.

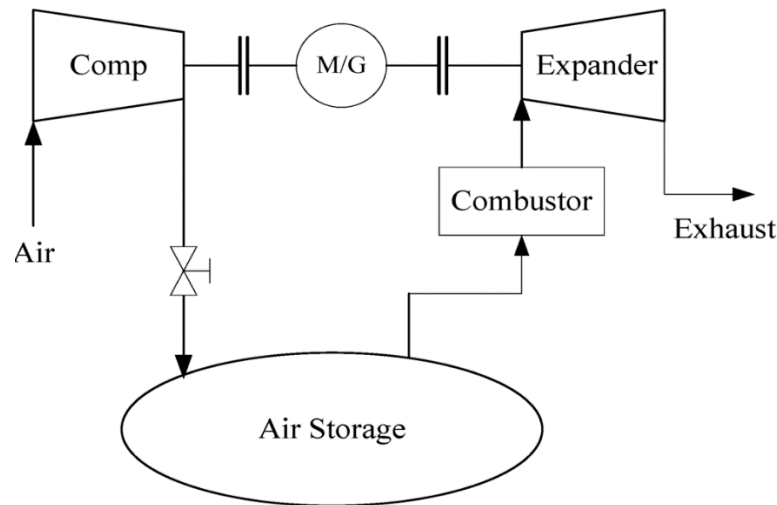


Figure 5. Schematic of a CAES power plant [8].

Along with pumped hydroelectricity storage, CAES is one of the largest energy storage technologies deployed to date. The first commercial CAES plant was the Huntorf plant in Germany. This plant could produce 290 MW for 2 hours of discharge, and started its operation in 1978 [9]. It was later modified to produce up to 320 MW with a round trip efficiency of 42%. The other large-scale CAES plant is in McIntosh, Alabama and has a rated power of 110 MW. This plant improved on the Huntorf design by incorporating a recuperator to preheat the air leaving the cavern using waste heat from the turbines. Despite the significant amount of research conducted on the various types of CAES systems (e.g. diabatic,



adiabatic and isothermal), there has been no large-scale deployment of this technology. However, with the rapid addition of intermittent renewable energy sources (e.g. wind and solar) to the grid, CAES is being perceived as a key enabler towards the development of a hybrid energy grid system.

### 3.1.2 Primary Model Design

As mentioned in the previous report, the operation of the turbomachinery components was based on performance maps that provide a relationship between the flow rate, pressure ratio and efficiency of the machinery involved [3]. The base model used for this analysis was acquired from the ThermoPower Library which employs the beta lines approach developed by Kurke [11]. This approach enables the user to tabulate the performance map data, which, via interpolation, can later be used to find the pressure ratio, flow number, and efficiency at a specific operating condition. The compressor model primarily on the beta lines method, whereas the turbine model uses only the rotational speed and pressure ratio to calculate the operating point.

The CAES model was split into two parts, one for each mode of operation: charging and discharging. Figure 6 shows the charging cycle of the CAES model, along with its control mechanism.

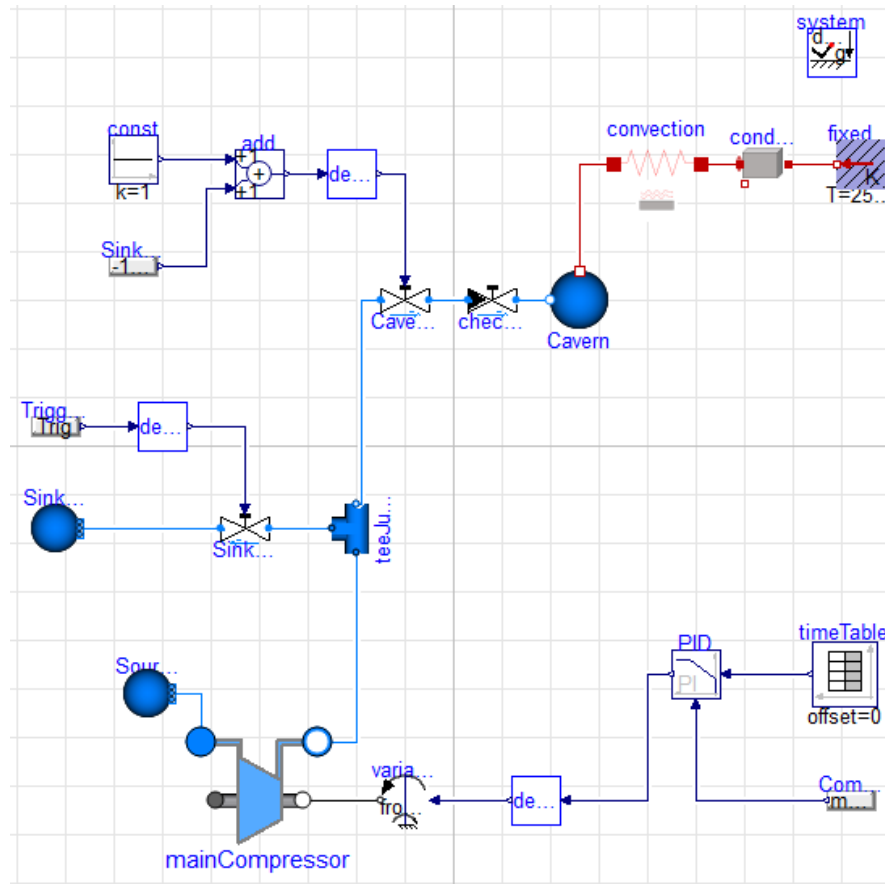
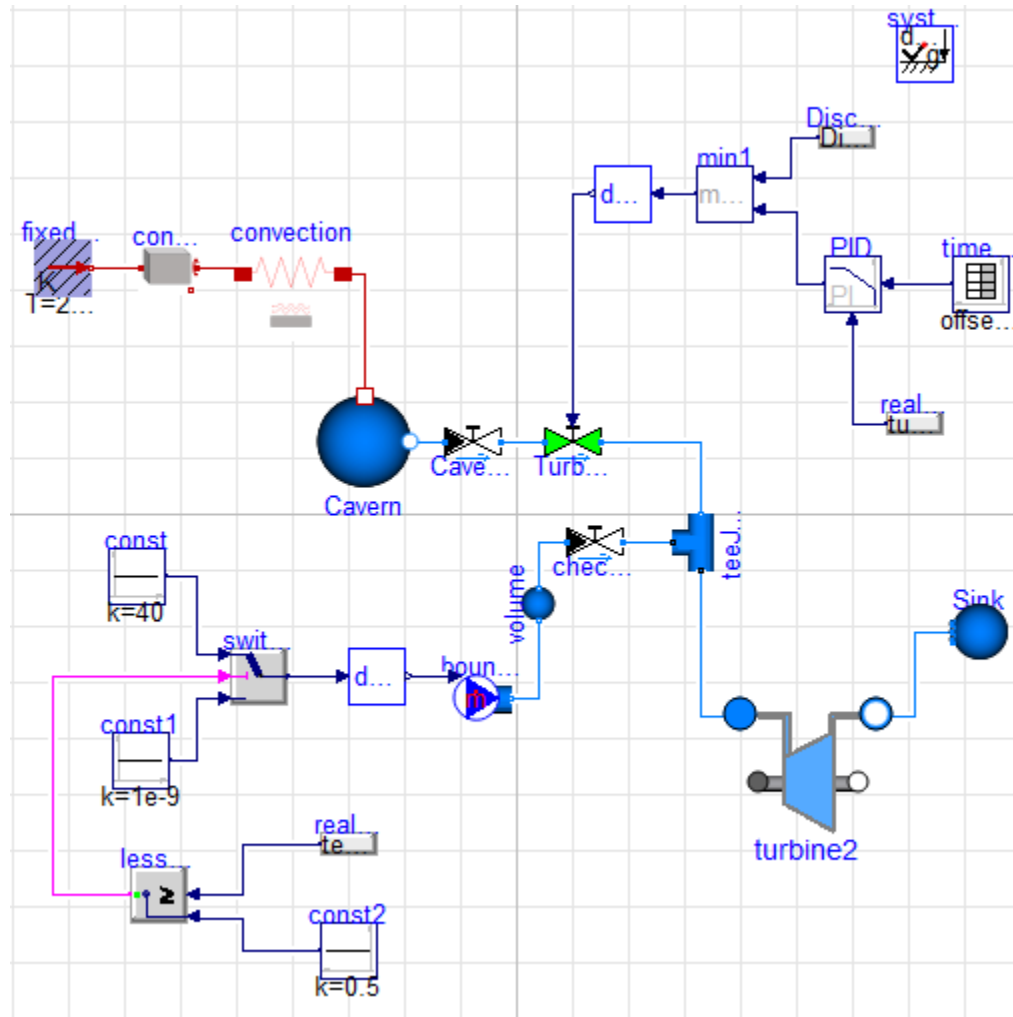


Figure 6. Charging cycle in the CAES model.

The compressor has a nominal design velocity of 1500 RPM (157.08 rad/s) but is controlled externally by a variable speed controller. A PI controller provides the input to the variable speed controller based on the goal of reducing the mismatch between the compressor power and the grid supply. For this model, the grid supply takes the form of a timetable. The cavern was designed using a simple volume of 1 million m<sup>3</sup>, along with a heat port to transfer heat to the surrounding cavern walls. The surrounding material is set to be solid rock, and heat transfer through it is modeled via a conduction

block. Appropriate thermal properties of the rock had to be provided, along with an ambient boundary condition temperature of 25°C.



The discharging cycle is currently modeled independently of charging-plus-storage model, primarily due to the limitations of the current turbomachinery components. The turbine used in the discharging cycle does not operate under zero flow conditions, which would occur in the turbine during the charging cycle. This issue can be overcome by combining the two models as sub-modules with logical connectors that trigger the charging and discharging cycles. This will be the focus of future work.

## 3.2 CAES Preliminary Results

Simulation results for charging and discharging modes compare to literature trends of similar models. These initial results are encouraging, and provide confidence that a full cycle model will provide realistic results.

### 3.2.1 Charging and Storage Mode

The current CAES charging model is set up to receive 125 MW of power from the grid during the charging cycle, store the compressed air for a period of 2 hours then depressurize the cavern to its minimum operating pressure in order to produce 125 MW of electricity during the discharging cycle. During the charging cycle, the compressor raises the cavern pressure from 18 bar to 26.5 bar a process that takes about 3.5 hours. The temperature of the compressed air also increases from 25 to about 112°C. Figure 8 shows the pressure and temperature profiles recorded during the charging cycle.

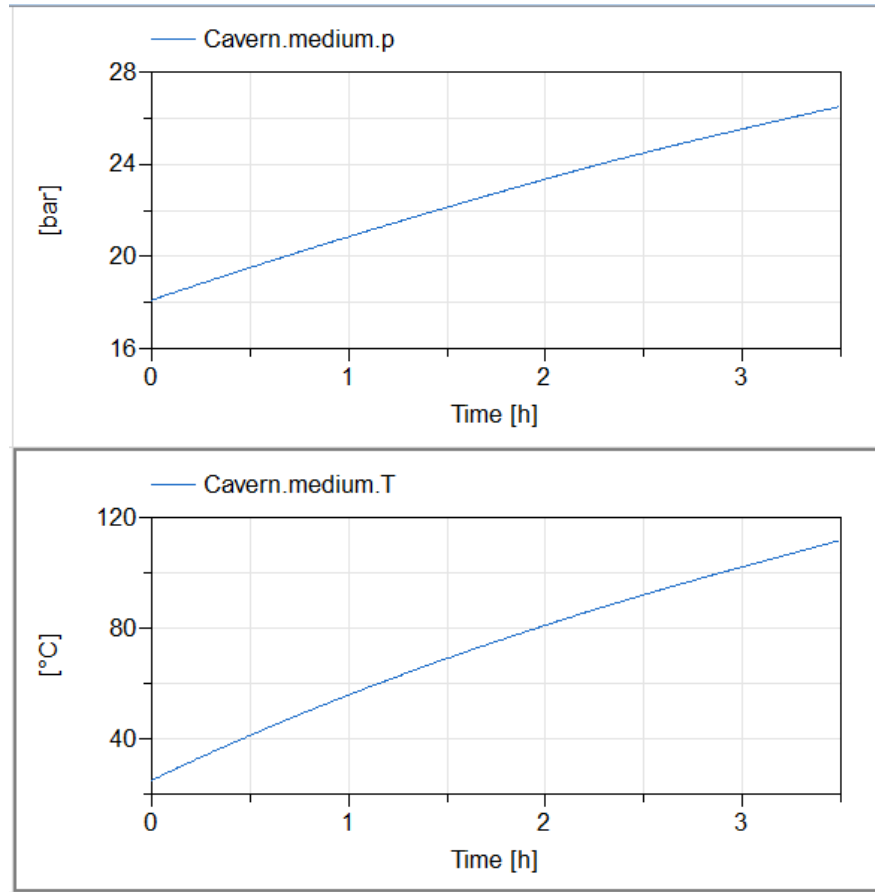


Figure 8. Cavern pressure and temperature during the charging cycle.

Once the cavern reaches this final pressure, the cavern valve is closed and a sink valve is opened to allow the compressor to dump the air to atmosphere, thereby preventing the compressor from dead-heading. During the storage period, loss of heat to the cavern walls causes the temperature of the air within the cavern to decrease along with the pressure. The heat loss from the cavern occurs both via convection and conduction. An average convective heat transfer coefficient of 25 W/m<sup>2</sup>-K was assumed for the air and the thermal conductivity of the surrounding rock was assumed to be 3 W/m-K. The surface area of the cavern was assumed to be 25000 m<sup>2</sup> and the thickness of the rock surface was assumed to be 1m, which was then subjected to a temperature boundary at 25°C. At the end of 2 hours of storage, the cavern pressure was 25.37 bar, and the air temperature 95.2°C. Figure 9 shows the temperature and pressure

profiles recorded during the storage mode.

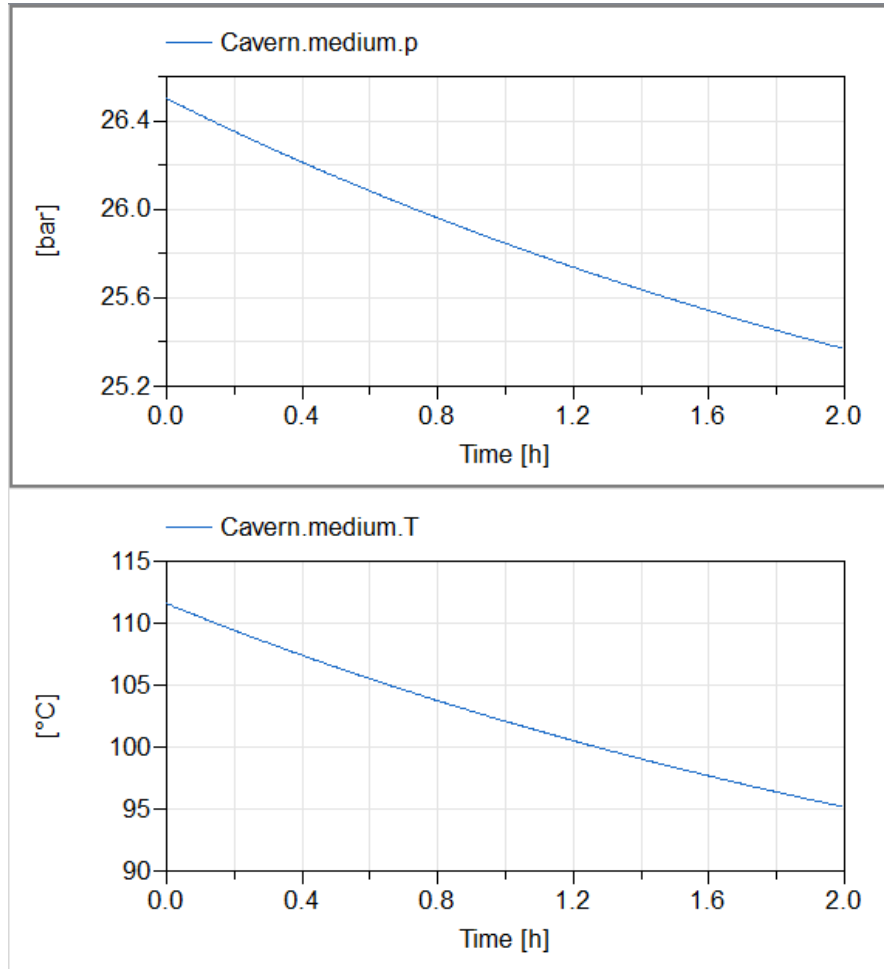


Figure 9. Pressure and temperature profile in the cavern during the storage mode.

### 3.2.2 Discharging Mode

The discharging cycle operates similar to the charging cycle; it uses an input signal from the grid to produce electricity by depressurizing the cavern and operating the turbine. The model is currently set up to discharge the cavern to produce 69.5 MW of electricity, at which point the cavern pressure decreases from 25.37 to 18 bar, and the temperature drops from 95.2 to 52°C. The discharge process takes about 3.5 hours. The overall round-trip efficiency is ~56%. Figure 10 shows the cavern pressure and temperature profile recorded during the discharging cycle.

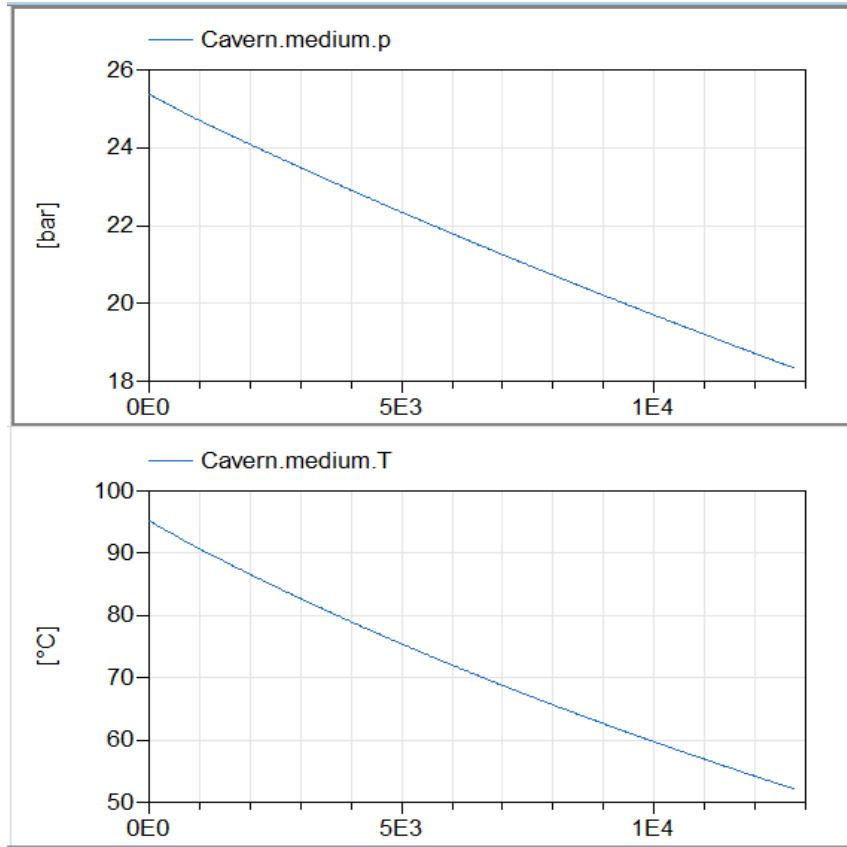


Figure 10. Cavern pressure and temperature profile during the discharge cycle.

### 3.3 Additional Planned Work

The current CAES model provides insight into the operation of the compressor and turbine when coupled to a fixed volume port. The relationship between the pressure and the mass flow rate from these turbomachinery components is very crucial to CAES system modeling and has been captured using the performance maps. However, several limitations to the model must still be overcome and will be the focus of future work.

The current model of the compressor starts directly at 100% of its nominal speed and can only operate down to 72% of this speed as and when the pressure ratio across it increases during the charging cycle. Also, the maximum pressure ratio deliverable by a single compressor is 32 at 105% of its nominal operating speed. When connected to an ambient pressure source, this results in the maximum achievable pressure of 32 bars, which is about half the operating pressure of existing CAES systems. Both of these aforementioned limitations primarily result from the data found in the compressor maps. To overcome these issues, new compressor map data must be added to the model along with a control scheme that enables the compressor to start from a lower nominal speed and reach a user-specified operational point.

A new control scheme is also needed to enable the compressor to slow down once the cavern reaches its maximum operating pressure and the cavern valve is closed. Currently, the compressor is connected to a sink- whose valve opens as and when the cavern valve closes. This prevents the compressor from dead-heading. During this switch from cavern to sink, the compressor still draws significant amount of power, which can be avoided if the compressor were to slow down its rotational speed.

Similarly, the discharging cycle operation is limited by the turbine performance map. Currently, the discharging cycle is separated from the charging cycle, mostly because the turbine does not operate at low mass flow rates, seen during the charging mode as well as once the discharge cycling is complete. Currently, an additional mass flow source is connected to the turbine that would provide a constant mass flow rate once the cavern reaches its final operating pressure and the discharge cycle is complete. This prevents the turbine model from operating in a regime that is unstable for it. The addition of a wider operating maps for the turbomachinery components will enable them to operate over larger flow and pressure ranges.

## **4. Two-Tank Sensible Heat Storage**

A two-tank sensible heat storage system exists in the HYBRID repository. The previous model was constructed using a large amount of custom modeling, with a significant amount of custom equation writing and algorithm use that may limit the ability to change the original two-tank model. With that in mind, an effort has been made to produce a similar system using HYBRID, TRANSFORM, and MSL components. One compelling reason to do so is to facilitate different storage heat applications. Altering the application of the stored energy should be facilitated by using common components.

### **4.1 Model Development**

To be considered complete, the two-tank model must be able to handle all storage operating modes, exchange different storage fluids (nominally Therminol-66 or a molten salt), and operate at relatively quick simulation speeds.

#### **4.1.1 Storage Two-Tank Loop Design**

Conceptualization of the components required for the two-tank loop design is straightforward. Two tanks, one hot and one cold, must be able to exchange fluids at controllable rates. Thus, the system operates by each tank having fluid pulled by pumps that direct flow through a control valve. After passing the control valve, the fluid flows through heat exchangers (either for charging or discharging) prior to entering the other tank.

The model requires the use of 1–3 fluid packages. The model allows for separate fluids to be defined for the charging/discharging fluids and the storage fluid. Up to this point, testing has been conducted using water as the charging/discharging fluid, condensing to store heat and boiling to withdraw it. So far, the modeling has primarily focused on an energy arbitrage concept: generating steam to produce electricity after storage.

Other types of energy applications and energy sources are possible. These could include various forms of single-phase heat applications, some feedstock preheating, or heat-boosting cryogenic boiling systems. Heat sources should be able to include integration with single-phase heat sources as well, such as a HTGR or perhaps molten-salt systems. The structure of the main two-tank sensible heat storage (SHS) model, Figure 11, should be as flexible as possible and allow control systems and outside model structures to determine the storage application.

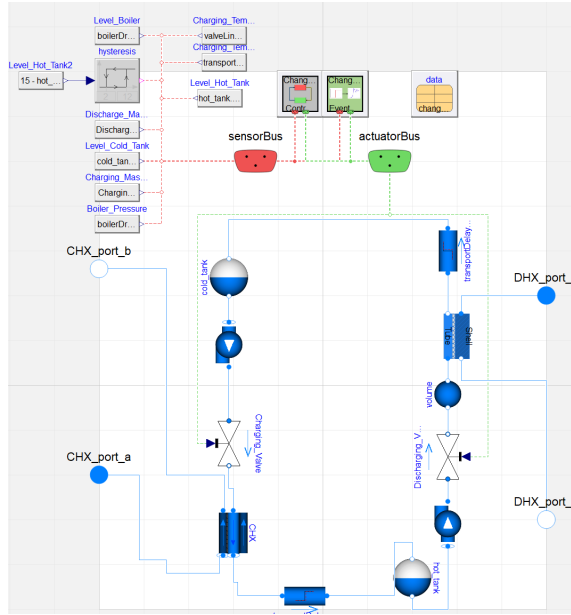


Figure 11. Model diagram of a sensible heat system.

Specific control of this type of system can be created in different models and exchanged as needed for analysis and application, one example is shown in Figure 12. However, one piece must be included for all control modes: namely, some manner of shutdown to ensure that neither tank is completely empties of its storage medium. This is done via the relatively complex appearing structure seen in the top two control methods. Rather than using a logic signal, a multiplier signal restricted to a  $[0,1]$  level multiplies with the standard PI control signal to force the valve to close or open smoothly and avoid simulation chattering. Note that this is a realistic requirement to ensure equipment safety.

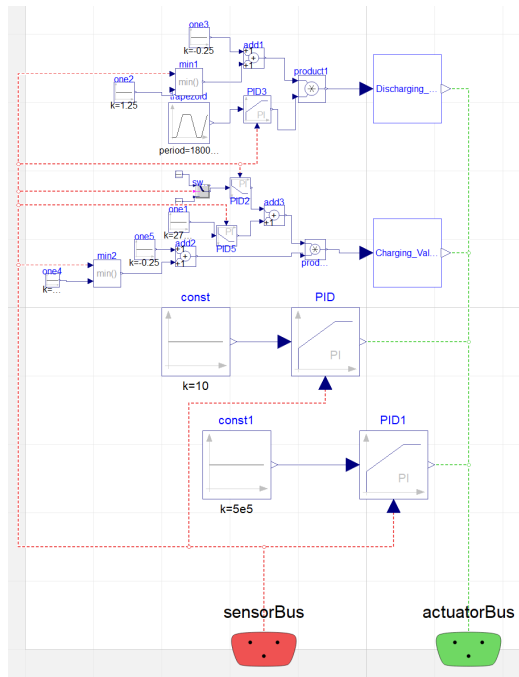


Figure 12. Control system model for the current standard SHS test.

The applied control system will be at least partially specific to the application. The charging valve control method should be consistent in maintaining a constant hot tank temperature. The discharging valve must be used to regulate the discharge power rate in some manner. When steam is produced, the steam mass flow rate may be the valid method. If a single-phase fluid is produced, discharging logic will likely be similar to the charging logic, with the SHS regulating the mass flow rate to produce the storage application flow rate and the application logic controlling the application's mass flow rate.

#### **4.1.2 Integration Design**

Integration with the charging and discharging heat methods is accomplished via heat exchanger. At present, one side of the two-tank model uses a common shell-and-tube heat exchanger, while the other uses a simplified heat exchanger.

The charging heat exchanger is nominally controlled to fill the storage whenever the hot tank fluid level drops to 2 m (15 m is maximum) and charging discontinues at 12 m. The nominal test uses this logic signal to initiate the outside steam flow in as well as a starter signal to initiate fluid movement from the cold tank to the hot tank. The charging control valve ensures that the temperature of the hot fluid sent to the hot tank meets a reference temperature. The mass flow rate is not specified, allowing it to float to any value such that the appropriate charging temperature is met.

In the nominal case, the discharging process is set up to produce steam at 5 bar. The application of the two-tank system heat may change in the future, so the nominal control scheme will likely change as well. In this case, a boiler model is constantly circulating liquid content through the discharging heat exchanger. The boiler has a pressure release valve set to its reference pressure (5 bar). The discharging control valve is controlled by the steam flow rate of this valve. When discharge is desired, the control valve will open until the steam demand is met.

### **4.2 Two-Tank Test Results**

#### **4.2.1 Stand-Alone System Results**

The system was tested as a stand-alone system. Some of the setpoints were mentioned in previous sections. The testing method was to produce 1.5 kg/s of 5 bar (70 psia) steam for 2.5 hours out of every 5 hours. Charging then occurred over whatever time duration was required to replenish the hot tank fluid level. A hysteresis controller initiated charging when the tank level dropped below 3 m and discontinued charging after the tank level reached 13 m. Figure 13 shows the tank levels. Decreases in the hot tank level and the corresponding rise in the cold tank level occur frequently as steam is produced from the boiler unit. The charging and discharging power rates can be seen in Figure 14. The system went through 48 discharging cycles and was in the middle of its 11<sup>th</sup> charging cycle when the simulation terminated. Overall, for this test, this means that 1 charging cycle could power around 4.5 discharging cycles. The fact that the charging cycles were initiated during different specific times of discharging cycles imparts a degree of robustness to the system testing.



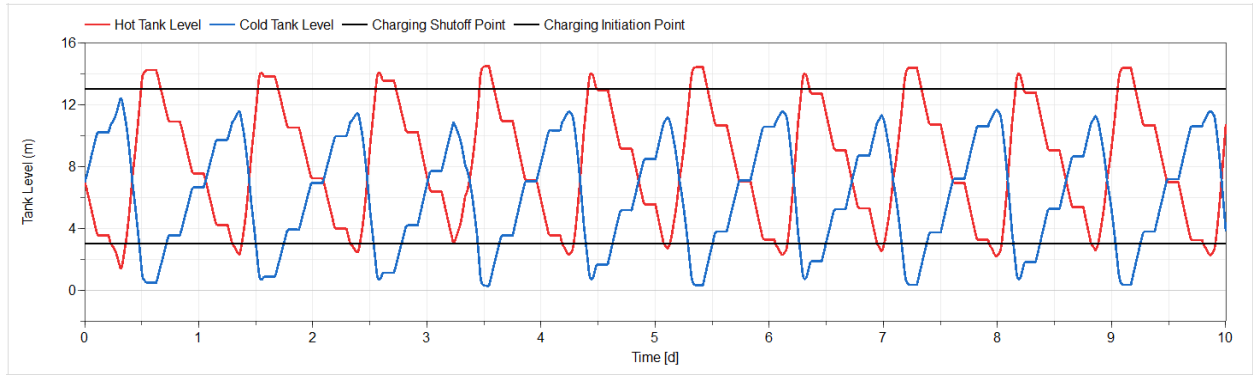


Figure 13. Hot and cold tank levels throughout the 10-day cycle. Hysteresis initiation and shutdown signals are included for reference.

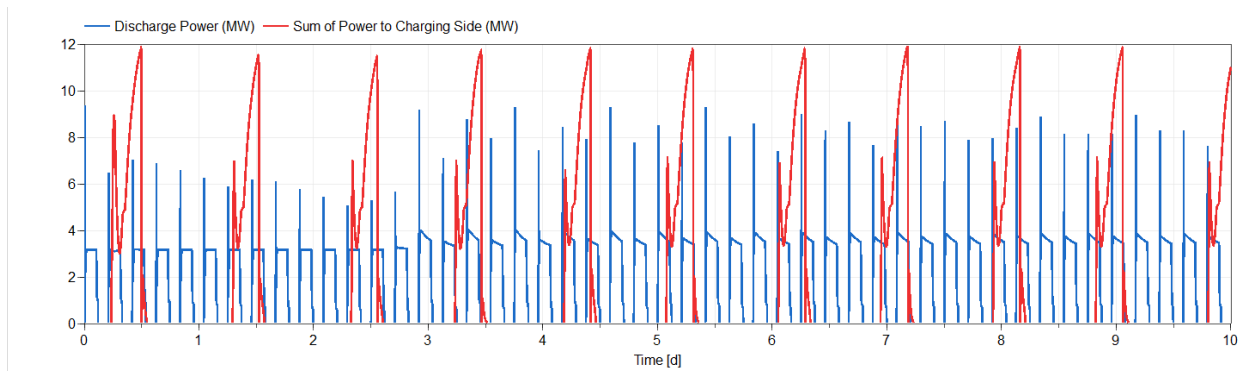


Figure 14. Discharging and charging power as measured within the heat exchangers.

The charging mass flow rate pattern is shown in Figure 15. This specific pattern, in which no steady-state charging flow is established indicates that the control system most likely needs to become more responsive to the measured conditions. The charging rate changes in response to the temperature of the storage medium entering the hot tank. A negative gain value is used, leading to an increased flow rate if the temperature exceeds the reference value. Additional testing should be conducted to determine if these charging mass flow shapes are simply a feature of the current control scheme or are simply the current controller gains.

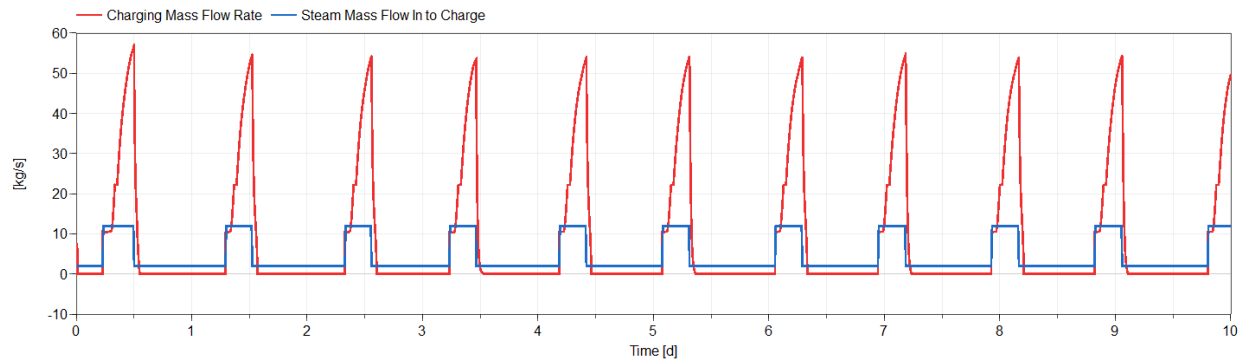


Figure 15. Charging mass flow rate on the storage side (red) along with the steam input (blue). Note that there is a 2 kg/s circulating flow on the steam side of the charging heat exchanger.

On the discharging side is found another very interesting type of behavior that a more advanced control scheme might successfully mitigate. A large burst of fluid appears both in the discharge mass flow rate and a corresponding mass flow rate exists in the steam discharge from the boiler (Figure 15 and

Figure 16). This is relatively common when valves are used with PI valves. If the time constants of the PI valves are much faster than those of the physics with which they interact, significant overshoot can occur. Additional controller tuning may be required (and possibly also the introduction of a “nominal” controller tuned to the specific deployment). Figure 17 shows the interaction between these two flow rates (by multiplying the steam rate in order to make them nearly even on the plot). The relatively long delay between the discharge mass flow rate increase and the steam flow rate increase might be decreased by reducing the volume of water in the discharge heat exchanger (leading to faster reactions in the boiler drum).

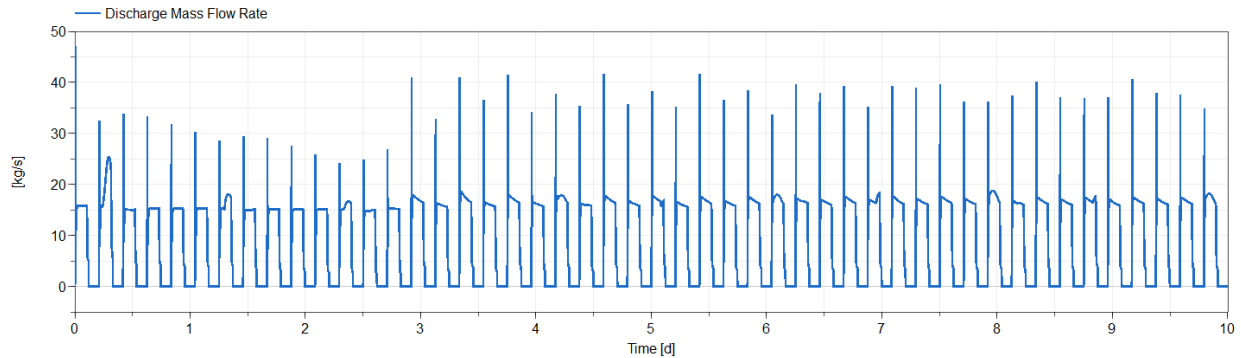


Figure 16. Discharge mass flow rate during the simulation.

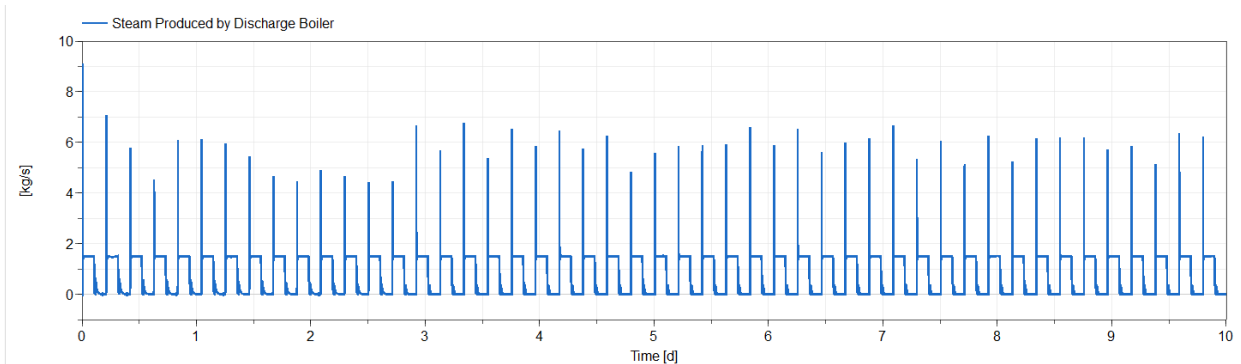


Figure 17. Steam production rate through the simulation. The demand during the discharging period is nominally 1.5kg/s.

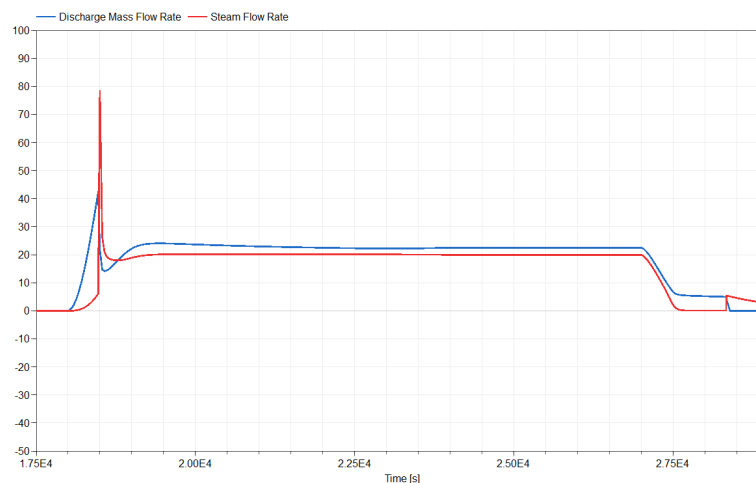


Figure 18. Discharge mass flow rate and normalized steam flow rate during a discharging cycle.

Figure 19 shows the hot/cold tank temperatures. It is clear from the cold tank temperature line that it is not fully constant, but does get to a relatively consistent cycle over the last few days. The cold tank temperature is not controlled in the system; however, if the saturation temperature of the boiler was shown, the cold tank temperature would be seen to be just a few degrees higher than the water saturation temperature. The hot tank temperature is constant except for at the beginning of charging cycles. This is due to the storage medium in the piping between the cold and hot tanks when charging initiates. While mass begins to flow, the heat flow does not immediately keep up, and so colder liquid is provided to the hot tank. Eventually, controller lag appears to raise the hot tank temperature slightly above the set temperature before ultimately settling at the nominal temperature.

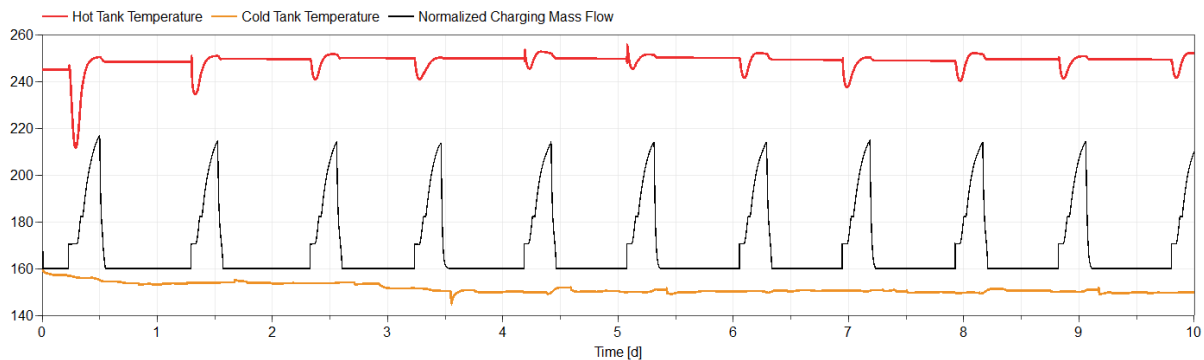


Figure 19. Hot and cold tank temperature profiles throughout the 10-day session. Charging mass flow is added (not-zeroed) to indicate charging periods.

Overall, the sensible two-tank system capable of passing through many charging, discharging, and standby cycles. Some improvements may be made in the future to increase the speed of the model. Additional control strategies for different deployment configurations should also be developed.

### 4.3 Additional Planned Work

The two-tank SHS system needs to be tested in additional applications. The HYBRID repository already contains multiple reactor models for integration with the system. Future reactor models may also include the SHS as an integral part of the design. This will require additional control system construction and energy application modeling.

Comparison validation testing should also be conducted to compare the newly constructed model with the original two-tank SHS model that already exists within the HYBRID repository. Both models already have access to the same media packages and the challenges will be to size the systems as identically as possible, as the construction of the models is quite different.

## 5. CONCLUSIONS

This report detailed the ongoing progress and future direction of adding to the HYBRID repository within FORCE. These tasks continue to support the goals and mission of the IES program at INL, through the development of programmatic capabilities for modeling and understanding a variety of potential IES deployment arrangements.

The HTGR, CAES, and SHS models have progressed to varying degrees of readiness for use in IES studies. Modelers believe that development is proceeding at a rate that will lead to the completion of the programmatic requirements. A high-level milestone report due in the summer of 2022 will provide a broader, clearer, picture of the overall status of the recent model construction in the HYBRID repository.

## 6. ACKNOWLEDGEMENTS

This work was supported by the IES program at INL under DOE Operations contract no. DE-AC07-05ID14517.

## 7. REFERENCES

- [1] Department of Energy. *Energy Storage Grand Challenge*. <https://www.energy.gov/energy-storage-grand-challenge/energy-storage-grand-challenge>. Accessed November 16, 2021.
- [2] Frick, K. and D. Mikkelsen. HYBRID. Updated April 6, 2022; cited April 13, 2022. Available: <https://www.github.com/idaholab/HYBRID>.
- [3] Mikkelsen, D., A. Shigrekar, K. Frick, and S. Bragg-Sitton. 2021. “Status Report on FY2022 Model Development within the Integrated Energy Systems HYBRID Repository. INL/EXT-21-65432, Idaho National Laboratory, Idaho Falls, ID. <https://doi.org/10.2172/1844226>.
- [4] Dassault Systems. DYMOLA Systems Engineering. Updated May 21, 2021; cited November 16, 2021. Available: <https://www.3ds.com/products-services/catia/products/dymola/>.
- [5] Modelica Association. “Modelica Standard Library.” Updated June 4, 2020; cited November 16, 2021. Available: <https://github.com/modelica/Modelica>.
- [6] Greenwood, M. S. 2017. “TRANSFORM - TRANSient Simulation Framework of Reconfigurable Models. Computer Software.” <https://github.com/ORNL-Modelica/TRANSFORM-Library>. November 7, 2017. eb. Oak Ridge National Laboratory. doi:10.11578/dc.20171109.1. Available: <https://github.com/ORNL-Modelica/TRANSFORM-Library>.
- [7] Brits, Y., F. Botha, H. van Antwerpen, and H. Chi. 2018. “A control approach investigation of the Xe-100 plant to perform load following within the operational range of 100 – 25 – 100%,” *Nuclear Engineering and Design*, 329, 12-19. <https://doi.org/10.1016/j.nucengdes.2017.11.041>.
- [8] Liu, W., L. Liu, G. Xu, F. Liang, Y. Yang, W. Zhang, and Y. Wu. 2014. “A Novel Hybrid-Fuel Storage System of Compressed Air Energy for China. *Energies*, 7(8), 4988-5010. <https://doi.org/10.3390/en7084988>.
- [9] Jafarizadeh, H., M. Soltani, and J. Nathwani. 2020. “Assessment of the Huntorf compressed air energy storage plant performance under enhanced modifications.” *Energy Conversion and Management*, 209, 112662. <https://doi.org/10.1016/j.enconman.2020.112662>.
- [10] Estill, J. 2008. Turbocharger Compressor Calculations. Accessed November 2021. <http://www.gnttype.org/techarea/turbo/turboflow.html>.
- [11] Sciacovelli, A., A. Vecchi, and Y. Ding. 2017. “Liquid air energy storage (LAES) with packed bed cold thermal storage – From component to system level performance through dynamic modeling,” *Applied Energy* 190, 84-98. <https://doi.org/10.1016/j.apenergy.2016.12.118>.